Leveraging Collagen-Mimetic Peptides for Modeling the Triple-Negative Breast Cancer Tumor Microenvironment

---

A thesis submitted by

Logan Dihanna Rubio

In partial fulfillment for the requirements for the degree of

Master of Science

In

Biomedical Engineering

Tufts University

May 2021

Advisor: Madeleine J. Oudin, PhD

Thesis Committee:
Madeleine J. Oudin, PhD
Qiaobing Xu, PhD
James Van Deventer, PhD

Abstract

Triple-negative breast cancer (TNBC) is an aggressive subtype of breast cancer with treatment options limited to cytotoxic chemotherapy. Given the morbidity of the disease, improved treatment options are required to improve patient outcomes. During TNBC progression, the collagen extracellular matrix is heavily remodeled by cells to promote tumor survival and metastasis. Collagen-mimetic peptides (CMPs) are synthetic collagen analogs that can be used to target areas of collagen remodeling. This project aims to explore how collagen is remodeled in a spheroid model of TNBC invasion, and if fluorescently-labeled CMPs can be targeted to these regions of high collagen remodeling in both fixed and live samples. Our results demonstrate that collagen is remodeled during TNBC spheroid invasion, and that CMPs hybridize into areas of collagen degradation in fixed TNBC spheroids. These results provide a framework to expand on leveraging CMPs in live samples.

Acknowledgements

First and foremost, to my advisor Dr. Madeleine Oudin, thank you for your guidance and support throughout my time at Tufts University. I appreciate you taking a chance on me with this project, and you have been a terrific role model both in and out of the lab. Your enthusiasm for this field is infectious, and I look forward to following the continued success of the Oudin Lab under your expertise. To my committee members, Dr. Qiabing Xu and Dr. James Van Deventer, thank you for the time and effort you have invested in supporting my project.

To the other members of the Oudin Lab, I have grown so much as a scientist through learning from each of you. Charlotte, your help in working through many aspects of this project with me and fielding even the smallest of questions has been invaluable. You are a fabulous scientist and I cannot wait to see where your time in the Oudin Lab takes you. To Victory and Priyanka, my fellow M.S. comrades, I am so thankful to have gone through this process with the two of you. I wish you both success in all of your future endeavors. To the rest of the lab, despite getting shut down halfway through my time with you, it has been a pleasure getting to know each of you and learning from your science. You have all truly left your mark on my time here at Tufts, and I will miss the lab dearly.

I would not be able to publish my science today if it were not for the tremendous support of Dr. Ellise Lamotte from the Center for STEM Diversity, and her role with the National GEM Consortium. Ellise, thank you for recognizing me as the daughter of an immigrant, and giving me the opportunity to follow my dreams as a researcher.

Finally, to my amazing family and friends, thank you for your patience and support. Mom and Dad, I am so lucky to feel your constant love and pride in my endeavors. I miss you

both every day, but I always cherish my trips home to Liverpool. To my brothers Leo and Lukas, you both inspire me to be the best that I can be, and I am so grateful for the bond that we share. I look forward to celebrating one another's greatest achievements throughout our lives. Finally, to Rob, thank you for always being there for me to lean on. You are an amazing friend and I am proud to be able to call you my colleague very soon. I surely would not be where I am today without you all.

Table of Contents

List of Figures

1 Introduction and Background

1.1 Introduction and Motivation

Triple-negative breast cancer (TNBC) is an aggressive and deadly disease that accounts for roughly 20% of breast cancer cases in the United States[1]. Five years post-diagnosis, TNBC patients with a localized tumor have a 91% survival rate compared to the general U.S. population[1]. However, for patients that experience metastasis, the dissemination of cancer cells from the primary tumor site, this statistic falls to 65%, and drops to just 11% for those that experience metastasis to distant organs[1]. Roughly 30% of breast cancer patients experience metastasis from the primary tumor either regionally or to organs such as brain, liver, lung, and bone, with TNBC representing a notoriously invasive subtype[1]. Additionally, Black and Hispanic populations have a greater chance of experiencing these more invasive forms of breast cancer[1].

Treatment options for TNBC patients include chemotherapy, radiation therapy, breast-conserving surgery, and partial or total mastectomy[1]. Unlike other molecular subtypes of breast cancer, TNBC lacks the three major cell receptors that can normally be targeted to inhibit tumor growth- those for the hormones estrogen and progesterone as well as those for human epidermal growth factor receptor 2 (HER2)[1]. As a result, treatment options for TNBC patients are restricted to systemic cytotoxic chemotherapy drugs with side effects including hair loss, weakened immune function, and organ damage. Given the severity of this disease and the lack of available treatment options, there is an imperative need for improved therapies to target TNBC.

The extracellular matrix (ECM) is a dynamic landscape of proteins which provide structural support to cells for adhesion and migration, as well as mechanical and chemical signals which regulate cell fate[2,3]. During TNBC progression, cancer cells work to facilitate a pro-tumor microenvironment that enables cell survival, proliferation, and migration[2–4]. The cells produce a variety of signals to initiate angiogenesis, or the development of new blood vasculature, as well as an inflammatory response, which in turn attracts immune and stromal cells to the tumor site[5]. In this tumor microenvironment, cells also coordinate the degradation and remodeling of the ECM through growth factors, protease activity and subsequent protein digestion[4,6]. As these ECM proteins are remodeled from a loose mesh network to dense, aligned fibers, the microenvironment becomes more conducive to tumor cell survival, proliferation, and metastasis[7,8]. Remodeling of the ECM therefore plays a significant role in the development and progression of TNBC[4].

Collagen is the most abundant ECM protein within the mammary tissue[9]. Mammary density, associated with collagen abundance and quantified by radiological density on a mammogram, is also associated with an increased risk of developing breast cancer[8,9]. Collagen remodeling in the TNBC tumor microenvironment involves the denaturation and fragmentation of the collagen protein, which is influenced by the presence of proteases whose enzymatic activity cleaves the collagen protein, followed by cellular internalization[4,6,10]. New collagen ECM is then deposited by cells to create a reorganized, highly aligned microenvironment to support malignant tumor progression[4]. This process is characterized by collagen deposition, crosslinking, and stiffening, which are ultimately associated with poorer prognoses and increased invasiveness in TNBC patients[7,11,12]. Extensive collagen turnover is a hallmark of TNBC as well as other disease states including cancer, inflammation, and fibrosis[4].

Collagen-mimetic peptides (CMPs), also known as collagen-hybridizing peptides, are a synthetic biomaterial developed based on the repeating amino acid sequence found in all collagens, typically $(Gly\text{-}Pro\text{-}X)_n$ or $(Gly\text{-}X\text{-}Hyp)_n$, where G represents glycine found at every third residue, followed by two amino acids where Pro denotes proline, Hyp denotes hydroxyproline, and X is any other amino acid residue[13,14]. These repeating subunits have the ability to self-assemble to form triple helices, the signature secondary protein structure known as tropocollagen, which gives rise to the hierarchical collagen structure found in tissue throughout the body[13]. By designing CMPs based on this repeating collagen motif, these synthetic peptides possess the natural capacity to hybridize into the backbone of endogenous collagen through a process called reversible strand invasion in order to form the complete triple helical structure[14]. As a tool for collagen identification in development, repair, and disease states, CMPs are highly sensitive and specific, detecting denatured collagen on the order of nanograms and discerning collagens from other ECM proteins or cell components[15].

Drug delivery systems (DDSs) are an exploding frontier in therapeutics, where biomaterials are designed to shuttle drugs for controlled release or improved targeting capabilities. By conjugating these drug vehicles with ECM-mimetic materials like CMPs, DDSs can not only enhance the targeting capabilities of therapeutics, but improve the retention and availability of therapeutics within the extracellular matrix in order to enhance the efficacy of treatments[16]. With the imperative need for targeted TNBC treatment options to prevent metastasis and improve patient outcomes, CMPs represent an emerging class of biomaterials that are being explored to leverage the ECM for improved targeting and controlled release of therapeutics.

This work aims to explore collagen remodeling within the context of *in vitro* TNBC models as a means to evaluate the targeting capability of CMPs in a simplified model of the TNBC tumor microenvironment. Using a 3D spheroid model of TNBC, which has been demonstrated in our lab as a predictive model of cancer cell invasion[17], I first evaluate collagen remodeling in response to cell invasion in spheroid models, and use this relationship to optimize the administration of CMPs by evaluating the hybridization of CMPs to areas of collagen degradation *in vitro*.

1.2 The Triple-Negative Breast Cancer Tumor Microenvironment

The architecture of human mammary tissue includes the nipples, ducts, and lobules that constitute the mammary gland, as well as the surrounding connective tissue, fat pad, and structural ligaments which physically support the tissue in combination with the pectoral muscles[18]. The mammary microenvironment is characterized by a variety of cells and interstitial proteins that make up the tissue. The epithelium is the monolayer of epithelial cells lining the inner glands, and is separated from the surrounding breast by the basement membrane, a specialized type of ECM that plays a role in tissue architecture, compartmentalization, filtration, and signaling[2]. The surrounding tissue is composed of stromal cells such as fibroblasts, adipocytes, vascular endothelial cells, innate immune cells such as macrophages and mast cells, and an ECM composed primarily of collagens, all together providing nutrients, immune defense, and structural support to the tissue[3]. Changes to the microenvironment during TNBC progression include the activation and recruitment of stromal and immune cell populations, and degradation and remodeling of the ECM, ultimately creating a pro-tumorigenic tissue microenvironment that supports outgrowth[2,8].

The cell-ECM interactions in mammary tissue are tightly coordinated and play a major role in mammary gland development as well as breast cancer progression by controlling aspects of cell proliferation, migration, and signaling[4]. TNBC tumor progression not only relies on alterations to cell processes, such as changes to cell cycle and metabolic pathways[5], but also on how a cell senses and responds to mechanical forces[19]. ECM components that are produced during both TNBC progression and mammary gland involution include fibrillar collagens, such as collagens I, III, and IV, which create a fibrotic stromal matrix, as well as ECM remodeling enzymes such as matrix metalloproteinases (MMPs) that not only aid in the reorganization of the ECM, but also release pro-tumorigenic ECM-derived growth factors[3,6]. The steps of metastasis, or the spread of cancer cells from a primary tumor, involve the local invasion to surrounding tissue, intravasation and travel through the vasculature, and colonization in distant organs[20]; this initial step of local invasion therefore relies heavily on cells' actuation of mechanical cues provided by the remodeled ECM[19].

1.3 Collagen Remodeling in Triple-Negative Breast Cancer

Collagen is a dynamic and highly abundant protein, with 28 various types accounting for roughly 25% of the total protein content in the human body[14]. Its signature hierarchal structure begins at the molecular level, where three collagen strands fold together to form stable right-handed triple helices[13]. These three strands contain identical or similar repeating amino acid sequences with glycine found at every third residue, denoted as $(Gly\text{-}X\text{-}Y)_n$[13]. The strands are also rich in proline and hydroxyproline, creating a semi-rigid backbone, and the repeating glycine residues give rise to the innate self-assembly of collagen molecules into triple-helices similar to that of DNA helices[13]. Collagen molecules form higher order structures, generating

microfibrils, which can bundle to form fibrils and eventually protein fibers through staggered, side-by-side molecular interactions[13]. During TNBC progression, collagen is denatured and fragmented into digestible pieces, and internalized by cancer and stromal cells which in turn deposit new collagen matrix as cancerous tissue[4,6].

Type I collagen in particular is significantly upregulated in the remodeled TNBC microenvironment[3]. An essential part of cancer infiltration and growth is disruption of the basement membrane, which cells achieve by producing MMPs to digest the collagen IV-rich basement membrane[6]. The basement membrane initially plays a role in suppressing tumor progression by controlling tissue architecture, but once disrupted leads to loss of epithelial cell polarity and thus emergence of the tumor phenotype[2]. This protease activity is also responsible for the continued denaturation and remodeling of interstitial collagen I to create a metastatic niche that allows cancer cells to survive, colonize, and proliferate[4]. The composition and organization of the newly deposited collagen matrix is influenced by this proteolytic digestion, as well as collagen deposition by cells and crosslinking of collagen, all which influence alignment and stiffening of the matrix[4,6]. As a result, high MMP expression correlates with poor prognosis and risk of recurrence, and collagen density and alignment is associated with increased cell invasiveness and poorer patient outcomes[4,7,8,12,21].

1.4 Collagen-Mimetic Peptides for Targeting Denatured Collagen

Collagen-mimetic peptides (CMPs), also known as collagen-hybridizing peptides, are a synthetic material with a design based on the natural collagen subunit. By incorporating the collagen motif, $(Gly\text{-}X\text{-}Y)_n$, into their design, these peptides maintain the natural ability to hybridize into the native collagen backbone to form stable structures by generating triple helices

with denatured collagen strands[14]. The melting temperature (T_m) of the peptide is controlled by the amino acid composition and length of the peptide design, with longer designs exhibiting higher melting temperatures[14]. Above this temperature CMPs will denature to generate individual CMP strands, and below the melting temperature, assemble to form triple helices either in homotrimers with each other in solution, or with denatured collagen when applied to tissues characterized by collagen damage or remodeling (Figure 1)[14,22,23]. While native collagen cannot return to 100% triple helical content after denaturation, the small size of CMPs allow for complete reversal of the triple helical assembly process through temperature cues[24].

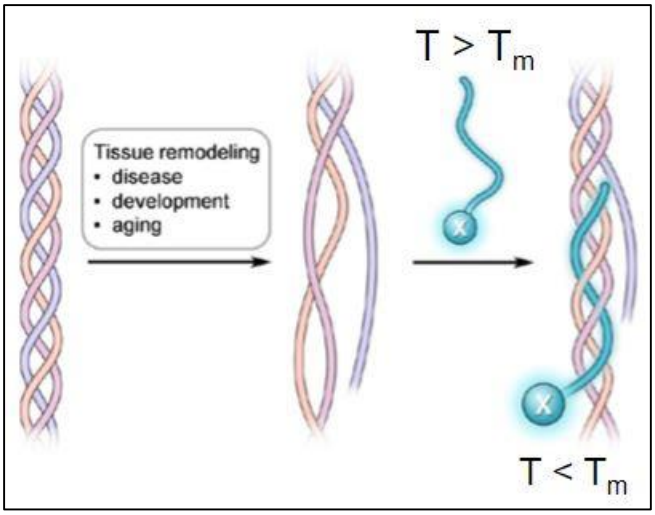

Figure 1 Reversible strand invasion process of collagen-mimetic peptides[25]

The capacity for triple helical assembly of CMPs can be leveraged to target areas of significant collagen turnover, where denatured collagen strands are exposed and available to CMPs for reversible strand invasion into the backbone of the tropocollagen molecule[14]. CMPs have been used in combination with fluorescent tags to target and visualize areas of collagen remodeling *in vitro*[23], *in situ*[26], and *in vivo*[15,27], where CMPs demonstrated accumulation to areas

of collagen turnover in development and disease states. Furthermore, the particular CMP design used in this study has been employed as a gene delivery vehicle by providing physical immobilization of DNA polyplexes to the collagen matrix, which demonstrated enhanced delivery of the polyplex based on subsequent gene expression by the cells, and further validated CMPs' collagen-targeting ability[28,29].

Finally, in combination with other biomaterials, CMPs can be utilized as drug-loaded, collagen-targeting nanoparticles. By conjugating CMPs with unique biomaterials that exhibit self-assembly into nanovesicles above their lower critical solution temperature, CMPs have been engineered as thermoresponsive self-assembled nanostructures capable of targeting collagen matrices[30,31]. This application highlights the long-term goal of applying CMPs as collagen-targeting nanoparticles for targeted therapeutics in the treatment of TNBC, which is hallmarked by significant collagen remodeling.

1.5 Conclusion

TNBC patients experience significantly more metastasis and morbidity compared to other breast cancer subtypes, and are more limited to non-specific cytotoxic chemotherapy for treatment. Beyond acting as a predictive marker of TNBC aggressiveness, the modified tumor ECM represents a dynamic protein landscape that can be leveraged for localized delivery of therapeutics. Given the significant extent of collagen remodeling occurring in the TNBC tumor microenvironment, therefore exposing the collagen backbone, CMPs may be useful for targeting areas characterized by significant collagen remodeling. With the long-term goal of applying collagen-targeting materials as drug delivery systems, this project aims to explore the

relationship between cancer cell invasion and collagen remodeling in order to assess the hybridization of CMPs in an *in vitro* model of the TNBC tumor microenvironment.

2 Quantifying Collagen Remodeling in Spheroid Models of Triple-Negative Breast Cancer Cell Invasion

In this chapter, I explore a common approach for assessing cancer cell invasion known as a spheroid invasion assay. By culturing TNBC cells embedded as spheroids in a collagen I gel, we can study collagen I remodeling by TNBC cells, namely the protease activity required to degrade the protein matrix and make way for cell invasion. Our lab's spheroid invasion model has previously been used to model spheroid invasion, but this work expands on our understanding of spheroid invasion to also model and quantify collagen degradation for a range of collagen I densities. The results of this chapter are used to visualize areas of collagen turnover in our TNBC spheroid model in order to predict where to expect hybridization of CMPs in Chapter 3.

2.1 Introduction

Breast tumor ECM is primarily composed of collagens, a structural ECM protein that influences cell behavior and communication through biomechanical and biochemical cues[3]. Cancer cells can migrate through tissue in an amoeboid-like style, where individual cells move through available spaces in the matrix, or by mesenchymal and collective cell invasion which require proteolytic degradation of the ECM[32]. Although the recruitment and activation of cancer-associated fibroblasts and immune cells are known to play a role in ECM remodeling through the indirect action of TNBC cells, whereby TNBC cell signaling induces upregulation of stromal-derived MMPs[10], the protease activity of the TNBC cells impacts ECM turnover directly, and has been shown to be upregulated in more invasive TNBC cell lines[33].

The spheroid assay is a standard method for assessing cancer cell 3D invasion, with more metastatic cancer cell lines invading further from the initial densely packed spheroid over the course of the culture period[17]. The assay has been utilized in mechanistic studies of migration as well in drug efficacy assessments due to the spheroid's ability to closely recapitulate *in vivo* cell mechanics and behavior[34].

These studies explore collagen remodeling *in vitro* in the context of breast cancer cell invasion. We utilize a spheroid model of a highly metastatic TNBC cell line known as MDA-MB-231s embedded in a collagen matrix to demonstrate the invasion of cells in 3D. By altering the collagen density, we demonstrate that matrix stiffness plays a role in modulating the invasiveness of breast cancer cells. Furthermore, we use a dye-quenchable collagen analog that fluoresces upon degradation to visualize collagen remodeling due to spheroid invasion. Together, these techniques are utilized to demonstrate that TNBC spheroid models can capture collagen I reorganization during cell invasion in an ECM density-dependent manner.

2.2 Methods

2.2.1 Cell Culture

The triple-negative breast cancer cell line MDA-MD-231 was obtained from American Type Cell Collection (Mannassas, VA) and previously engineered to express red fluorescent protein (RFP) through lentiviral infection. Cells were thawed and cultured on uncoated tissue culture plastic in culture medium containing Dulbecco's modified Eagle's medium (DMEM) supplemented with 10% fetal bovine serum (SH30071.03; Cytiva; Marlborough, MA) and 1% penicillin-streptomycin-glutamine (10378016; ThermoFisher Scientific; Waltham, MA). Cultures were routinely tested for mycoplasma contamination using a Universal Mycoplasma

Detection Kit (30-1012K; ATCC; Manassas, VA) and used between p5 and p20 for all experiments.

2.2.2 Spheroid Invasion Assay

Spheroid invasion assays were performed as described previously[35]. 1,000 RFP-expressing MDA-MB-231 cells were seeded in culture media in an ultra-low attachment, round-bottom 96-well spheroid microplate (4515; Corning; Corning, NY) and centrifuged at 3,000 g for 8 min to create a densely packed spheroid of cells. After 3 days in culture, spheroids were imaged as a Z-stack using a Keyence BZ-X710 microscope (Keyence, Elmwood Park, NJ) with a TxRed filter cube to obtain initial spheroid size (day 0). 1, 2, 4, and 6 mg/mL collagen I gel mixtures were created using a combination of high-concentration rat tail collagen I protein (354249; Corning; Corning, NY), 10mM NaOH, 7.5% 10X DMEM, and culture media, and added to the wells. The plate was centrifuged again at 3,000 g for 10 min to pack the ECM mixture around the spheroid, and allowed to polymerize at 37°C. After 2 hr, 50 µL of culture media was added to the gels to prevent gel shrinkage and maintain moisture. Spheroids were kept in culture for several days and imaged as a Z-stack again on day 4 to capture spheroid invasion into the collagen gel.

2.2.3 Dye-Quenched Collagen I Assay

FITC dye-quenched collagen I (DQ-Col1) from bovine skin (D12060; ThermoFisher Scientific; Waltham, MA) was utilized as a component of the ECM mixture in our spheroid invasion assays in order to visualize collagen I cleavage. 0, 2, or 4% (w/w) of the collagen I content in 1, 2, and 4 mg/mL gels was substituted for FITC-DQ-Col1 in order to maintain the density of the collagen gels for a given concentration. FITC-DQ-Col1 was also incorporated into

no cell control collagen I gels. Samples were kept in culture over several days and imaged as a Z-stack using a Keyence BZ-X710 microscope with TxRed and GFP filter cubes on day 4 to capture the RFP and FITC signals.

2.2.4 Spheroid Invasion Analysis

Images were processed and analyzed using ImageJ. Z-stacks were projected into single images based on the maximum intensity from each slice of the stack. The RFP signal was adjusted and thresholded to generate a binary mask of the cancer cell spheroid, and the ROI manager in ImageJ was used to record the locations of each cell or region of cells. The distance from the center of the spheroid area was calculated for each ROI, and data is expressed as the cumulative distribution of ROIs from the spheroid core, the standard deviation of the distribution, and the average of the 10 furthest ROIs from the spheroid core.

2.2.5 Dye-Quenched Collagen I Analysis

Using the ROIs obtained from the cell invasion analysis, the mean FITC signal intensity was measured at each ROI and normalized to the area of the ROI. Additionally, the background FITC-DQ-Col1 signal from the no cell control conditions was subtracted from the normalized FITC signal intensity for spheroid conditions in order to generate a normalized FITC intensity resulting from cell activity.

2.2.6 Statistical Analysis

Statistical significance was determined by one-way ANOVA, and results were considered statistically significant for $p < 0.05$. Analysis and data visualization were performed in GraphPad Prism 8.3.1.

2.3 Results

2.3.1 Cancer Cell Spheroid Invasion is Modulated by Collagen Density

I was interested in understanding if collagen density influenced TNBC cell invasion given its role in mediating metabolism[21], migration[12], and overall patient prognosis[11]. To this end, I established a simplified *in vitro* model of the TNBC tumor microenvironment by embedding a spheroid of highly metastatic MDA-MB-231 cells in a range of collagen I densities. After 4 days of incubation, MDA-MB-231 cells invaded from the initial spheroid into the surrounding collagen gel (Figure 2A). The cumulative distribution of the distance of cells from the spheroid core tended to increase as collagen I density increased, indicating that peripheral cells were collectively traveling further from the spheroid core (Figure 2B). As collagen density increased, the standard deviation of the cell distribution from the spheroid core and the average maximum distance of the cell distribution also increased (Figure 2C, 2D). This finding was significantly different for the 6 mg/mL collagen I density relative to the 1, 2, and 4 mg/mL gels. These results show that increased collagen density can promote TNBC cell invasion.

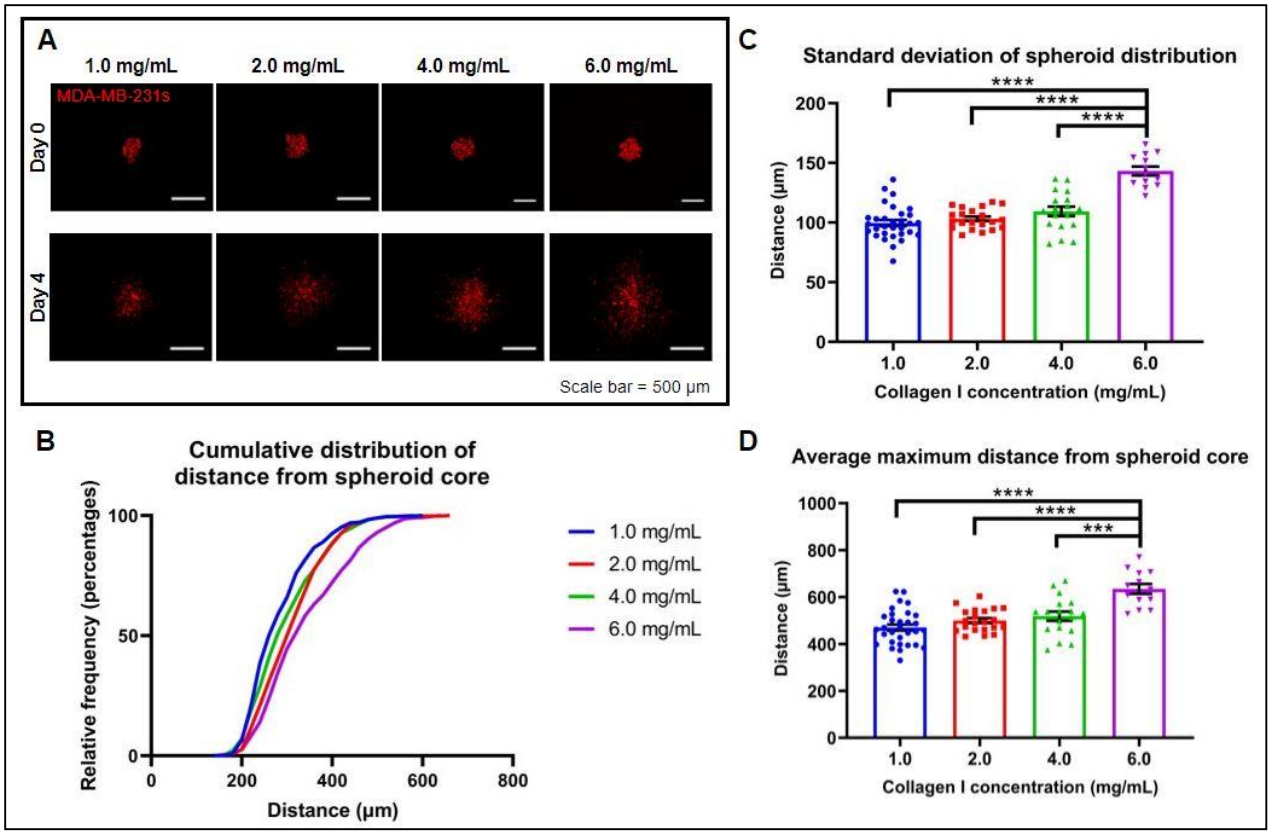

Figure 2 Increasing collagen I density promotes TNBC spheroid invasion

(A) Representative images of RFP MDA-MB-231 spheroid invasion into surrounding matrix from day 0 to day 4 for 1, 2, 4, and 6 mg/mL collagen I gels. (B) Cumulative distribution of cell distances from spheroid core in 1, 2, 4, and 6 mg/mL collagen I gels on day 4 of spheroid culture. (C) Standard deviation of spheroid distribution from core in 1, 2, 4, and 6 mg/mL collagen I gels on day 4 of spheroid culture. (D) Average of 10 furthest points from spheroid core in 1, 2, 4, and 6 mg/mL collagen I gels on day 4 of spheroid culture. Data represents group means ± standard error of measurement with n = 3 biological replicates. Statistical significance ($p < 0.001$ or $p = 0.001$) from a one-way ANOVA is indicated by **** or ***, respectively.

2.3.2 Collagen Degradation is Modulated by Collagen Density

Previously, our lab's TNBC spheroid model has been used to visualize and quantify cell invasive potential. I was interested in using this model to assess collagen degradation in addition to spheroid invasion. In order to explore the relationship between cancer cell invasion and collagen degradation, I utilized a dye-quenched collagen I analog (DQ-Col1) that fluoresces

upon degradation. We incorporated DQ-Col1 into the collagen matrix at 2 and 4% of total collagen I (w/w) to determine whether collagen degradation as a result of cancer cell invasion into the surrounding matrix could be measured using the DQ-Col1 fluorescent signal. As shown in Figure 3A, at lower collagen I densities of 1 and 2 mg/mL, the FITC signal from the DQ-Col1 was not significantly different from the 0% DQ-Col1 control condition. However, for a 4 mg/mL gel, 4% DQ-Col1 showed significantly elevated fluorescent intensity relative to the control condition. Unlike our previous result, there was no increase in invasion with increased collagen density, and our metrics of spheroid invasion actually demonstrated a decrease in invasion for 4 mg/mL collagen gels relative to 1 and 2 mg/mL collagen gels (Figure 3B, 3C). This result indicates that despite the metrics of spheroid invasion indicating less migration into the collagen matrix as collagen density increases, the DQ-Col1 signal captures an increase in collagen remodeling for denser collagen gels.

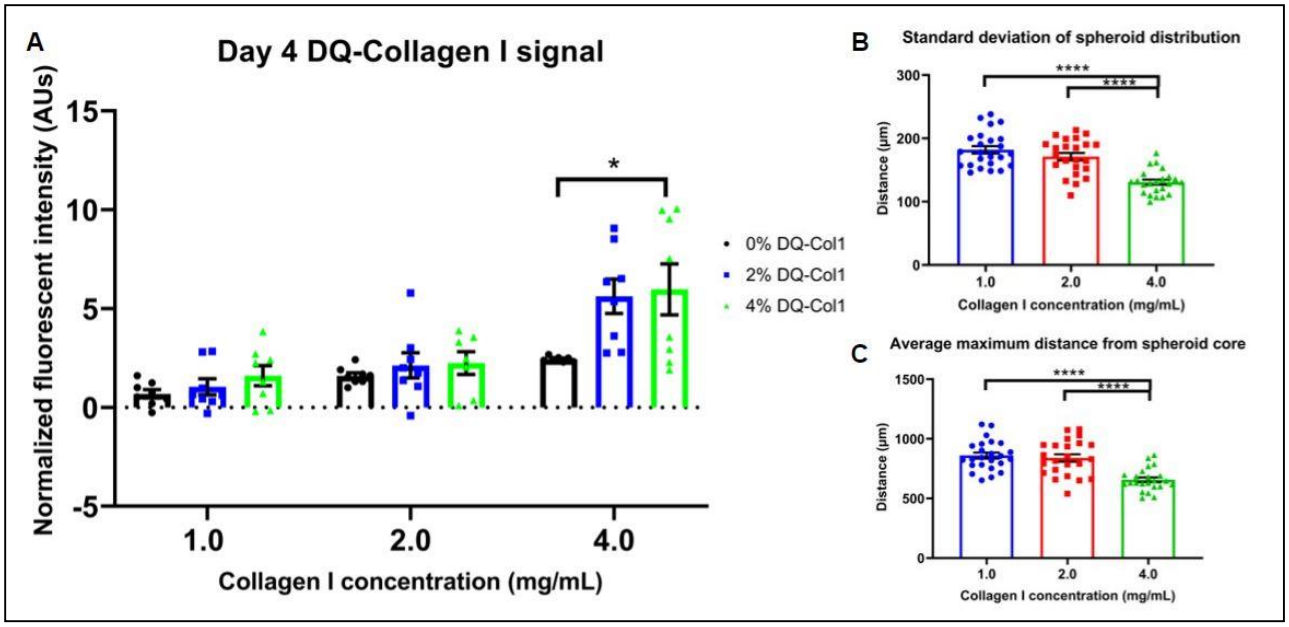

Figure 3 Dye-quenched collagen I captures collagen remodeling in high-density collagen I gels

(A) Normalized fluorescent intensity of 0, 2, and 4% FITC DQ-Col1 signal in 1, 2, and 4 mg/mL collagen I gels on day 4 of spheroid culture. (B) Standard deviation of spheroid distribution from core for 0, 2 and 4% FITC DQ-Col1 conditions in 1, 2, and 4 mg/mL collagen I gels on day 4 of spheroid culture. (C) Average of 10 furthest points from spheroid core for 0, 2, and 4% FITC DQ-Col1 conditions in 1, 2, and 4 mg/mL collagen I gels on day 4 of spheroid culture. Data represents group means ± standard error of measurement with n = 2 biological replicates. Statistical significance ($p < 0.05$ or $p < 0.0001$) from a one-way ANOVA is indicated by * or ****, respectively.

2.4 Discussion

The TNBC tumor microenvironment is a highly dynamic and heterogeneous landscape of cells and proteins. The first step in replicating cell-ECM interactions *in vitro* requires simplified models, and this particular approach focused directly on TNBC cells and their interactions with collagen I protein in a 3D matrix in order to capture cell invasion and proteolytic remodeling. Although collagen matrix stiffness and crosslinking is associated with poorer patient outcomes[8,11], it is unclear exactly how cancer cells alone respond to denser collagen matrices *in*

vitro on a shortened timescale in the absence of stromal cells that are known to play a major role in collagen remodeling. Furthermore, variabilities in a pure collagen I matrix can arise as a result of inconsistencies in the triple-helical content of a given collagen I solution, changes in pH and temperature during polymerization, as well as the pore size and fiber alignment of the polymerized gel. In addition, the different sources of our collagen I (rat tail) versus our DQ-Col1 (bovine skin) could result in inconsistencies between conditions due to differences in stiffness, or post-translational modification of the collagen. Ultimately, the spheroid invasion assay employed herein provides a platform for assessing both cancer cell invasion and collagen remodeling, but variabilities between experiments are abundant as demonstrated in these results. Despite these variabilities, it is clear that changes in collagen I density play a role in modulating cancer cell invasion, and that increasing collagen I density influences the extent of collagen degradation occurring for a given spheroid.

Examining multiple metrics of cell invasion is pertinent for this setup due to the nature of individual versus collective cell invasion. Cancer cells are able to migrate individually in an amoeboid-like manner in which cells move through the smallest pores of a matrix[32]. Additionally, it has been demonstrated that collective cell invasion relies on significant proteolytic activity to degrade the surrounding ECM, which involves a range of proteases including MMPs[32]. This project aimed to explore the relationship between cancer cell invasion and collagen degradation, and focused on collective cell migration due to proteolytic activity in order to capture areas of collagen remodeling as a biomarker of TNBC. Previously, our lab has quantified the fold change in spheroid area as a metric of cell invasion; since spheroid area can be affected by cell proliferation, however, I decided instead to look at the distribution of individual cells or regions of cells from the spheroid core and the average maximum distance

traveled by a single cell within a spheroid in order to capture the full range of invasion types that occurred for a given spheroid. Together, these metrics are used to assess spheroid invasion at various levels in order to understand how spheroid invasion relates to collagen degradation, and where in relation to the spheroid to expect significant collagen remodeling.

Previously, DQ-Col1 has been used in combination with MDA-MB-231 cells in a model of individual cell invasion through a 3D collagen matrix, in which cells were dispersed cells throughout the matrix and allowed the gel to polymerize[23], as well as to model collagen remodeling around a spheroid of MDA-MB-231s[32]. Both of these models, however, focused on imaging pericellular collagen remodeling in the vicinity of single MDA-MB-231 cells. The later also measured the DQ-Col1 signal as it was released into the supernatant rather than measuring DQ-Col1 fluorescence directly from imaging. Thus, we set out to determine an optimal concentration for capturing collagen remodeling for an entire spheroid for a range of collagen I densities. Although it has been shown that collective cell invasion requires collagen remodeling[32], the DQ-Col1 signal was insignificant relative to the control conditions at lower collagen densities despite obvious spheroid invasion into the matrix. This finding is consistent with previous literature which describes protease-dependent migration as more important for invasion in higher density collagen gels, whereas in lower density gels cells can invade through larger pores in the matrix[36]. Further assessment of this result work is warranted in order to determine the mode of invasion for cells depending on matrix stiffness. Nonetheless, the fluorescent signal was significantly enhanced for the 4% DQ-Col1 condition in a 4 mg/mL collagen gel, indicating that our spheroid model captures significant collagen degradation in high density collagen gels. This result suggests that although stiffer matrices have a variable effect on cancer cell invasion, they do in fact trigger elevated levels of collagen degradation.

2.5 Conclusion

TNBC cells are known to interact extensively with the surrounding extracellular matrix in order to create a pro-tumorigenic microenvironment. I employed a simplified model of the TNBC tumor microenvironment using MDA-MB-231 cells in a collagen I matrix to determine the relationship between collagen I remodeling and TNBC cell invasion. Despite variabilities in the collagen matrices, it is clear that collagen density plays a role in modulating the extent of cancer cell invasion as well as collagen remodeling. Furthermore, a common tool known as dye-quenched collagen I used to visualize collagen degradation was employed to examine the levels of collagen remodeling in response to spheroid invasion within a range of collagen densities. The DQ-Col1 signal revealed that higher density collagen I gels promoted collagen remodeling *in vitro*. Together, these data provide an avenue for assessing collagen remodeling in the context of TNBC spheroid invasion, and can be used as a benchmark for assessing the targeting ability of CMPs.

3 Integration of Fluorescently-labeled Collagen-mimetic Peptides into Spheroid Models of Cell Invasion

In this chapter, I explore the hybridization of a fluorescently-tagged collagen-mimetic peptide (CMP) design applied to our standard spheroid assay. I examine the effects of the peptide on cell invasion, and assess the hybridization of the peptide in various settings according to temperature, cell activity, and extent of collagen remodeling. Furthermore, I examine the signal accumulation in the vicinity of the spheroid. Together, these results aim to integrate the administration of CMPs into our spheroid setup in order to assess the targeting ability of CMPs in the context of TNBC tumors.

3.1 Introduction

Fluorescently-labeled CMPs have been used to target tissues undergoing significant collagen remodeling[14,23,26]. These peptides are specifically engineered to exhibit reversible trimerizing behavior above a given melting temperature (T_m) based on their amino acid sequence and length[14]. CMPs have demonstrated specificity for various types of collagen with no affinity for non-collagenous ECM proteins or cell lysate, as well as sensitivity down to roughly 5 ng[15].

The amino acid sequence of the CMP design used herein is CF-$(GPP)_3$GPRGEKGERGPR$(GPP)_3$GPCCG, where CF represents a tethered carboxyfluorescein molecule, and the melting temperature of the design is 52°C. The fluorophore has a peak excitation and emission spectra of 489 and 533 nm, respectively. This CMP design has been used in studies of gene delivery, where CMPs have been shown to enhance delivery and uptake of DNA polyplexes through physical immobilization to collagen matrices[28,29]. Previously, similar

CMP designs have been applied to TNBC models to visualize collagen turnover in fixed samples[23]. These studies have demonstrated the localization of the peptide around cell tracks in a 3D model of individual cell migration, but to my knowledge have not been applied to spheroid models of TNBC.

In this study, fluorescently-labeled CMPs are employed to our tunable TNBC tumor spheroid model. I use the CMPs pre-incubated with our collagen matrices in a spheroid model to assess the effects of CMP presence on breast cancer cell invasion over the course of the culture period. I then apply CMPs to breast cancer spheroids with varying degrees of collagen remodeling in fixed and live samples in order to assess the capacity for CMP hybridization. The results demonstrate that CMPs hybridize to areas of collagen turnover in fixed spheroid samples, and that their application in live spheroids requires optimization to determine a sufficient temperature level that cells can survive at while providing a temperature cue for the CMPs to fold into triple helices. Broadly, this work lays the foundation for examining the interactions between CMPs and live cells *in vitro* in order assess the delivery and retention of CMPs to tumor sites.

3.2 Methods

3.2.1 Pre-incubation of Collagen-Mimetic Peptides

For studies of CF-CMP effects on spheroid invasion, CF-CMPs were pre-incubated with collagen I prior to adding the ECM mixture to the spheroids. 0, 0.05, and 0.1% (w/w) of the collagen I content in 1, 2, and 4 mg/mL gels was substituted for CF-CMPs in order to maintain the density of the collagen gels for a given concentration. A 50 mM CF-CMP solution in MDA-MB-231 cell culture media was generated in a roughly 30 µL volume to be administered to pure

collagen I solutions. The CF-CMP solution was first heated for 5 min at 65°C to thermally dissociate any self-trimerized peptides into individual CF-CMP strands, followed by cold quenching and rapid mixing in an ice bath for roughly 10 sec to room temperature to administer to collagen I solutions. Collagen I and CF-CMP mixtures were thoroughly mixed and incubated for 2 hr at 4°C in order to allow CF-CMPs to integrate into the collagen I backbone without gelation of the solution. The mixture was then added to the standard ECM mixture containing 10mM NaOH, 7.5% 10X DMEM, and culture media, added to spheroids, and allowed to polymerize at 37°C. Spheroids were kept in culture for several days and imaged as a Z-stack on day 4 to capture spheroid invasion into the collagen gel with and without the addition of CF-CMPs.

3.2.2 Spheroid Gel Fixation

MDA-MB-231 cells were cultured in spheroids as described in Chapter 2. On day 4 of growth, spheroids were transferred to a 12-well plate and submerged in 2 mL of 2% paraformaldehyde in 1x phosphate buffer saline (PBS). Samples were fixed statically for 10 min at room temperature, followed by 10 min on a rocker at room temperature. After fixation, samples were washed 3 times in PBS for 5 min each, and stored at 4°C in PBS until use.

3.2.3 Administration of Collagen-Mimetic Peptides to Fixed Samples

A stock solution of carboxyfluorescein-tethered collagen-mimetic peptides (CF-CMPs) in DI water was supplied in collaboration from the lab of Dr. Millicent Sullivan at the University of Delaware (Newark, Delaware). CF-CMP solutions were generated in roughly 600 µL volumes in PBS to be administered to fixed wells at 0 mM and 5 mM concentrations. Solutions were first heated for 5 min at 65°C to thermally dissociate any self-trimerized peptides into individual CF-

CMP strands, followed by cold quenching and rapid mixing in an ice bath for roughly 20 sec to room temperature to administer to wells. Fixed gels were transferred from a 12-well plate to a 96-well plate. 100 µL of either the 0 mM or 5 mM CF-CMP solutions was administered to each well and incubated at 4°C for 2 hr. The solutions were also administered to no cell control fixed collagen I gels. All samples were then transferred to a 12-well plate and thoroughly washed with PBS 3 times for 30 min each at room temperature. Samples were then transferred to a 96-well glass bottom plate and each sample was imaged as a Z-stack using a Keyence BZ-X710 microscope with TxRed and GFP filter cubes to capture the RFP and CF signals.

3.2.4 Administration of Collagen-Mimetic Peptides to Live Samples

CF-CMP solutions were generated in roughly 600 µL volumes in MDA-MB-231 cell culture media to be administered to live wells at 0 mM and 5 mM concentrations. Solutions were first heated for 5 min at 65°C to thermally dissociate any self-trimerized peptides into individual CF-CMP strands, followed by cold quenching and rapid mixing in an ice bath for roughly 20 sec to room temperature to administer to wells. 50 µL of MDA-MB-231 cell culture media was removed from live spheroid and no cell control samples. 100 µL of either the 0 mM or 5 mM CF-CMP solutions was administered to each well of a 96-well plate and incubated at 37°C for 2-24 hr. The solutions were also administered to no cell control collagen I gels. All samples were then transferred to a 12-well plate and thoroughly washed with MDA-MB-231 cell culture media 3 times for 30 min each at 37°C. Samples were then transferred to a 96-well glass bottom plate and each sample was imaged as a Z-stack using a Keyence BZ-X710 microscope with TxRed and GFP filter cubes to capture the RFP and CF signals.

3.2.5 Collagen-Mimetic Peptide Signal Analysis

Spheroid invasion was assessed as described in Chapter 2. Briefly, image Z-stacks were projected into single images based on the maximum intensity from each slice of the stack. A binary mask of the cancer cell spheroid was used with the ROI manager in ImageJ to record the locations of each cell or region of cells. The distance from the center of the spheroid area was calculated for each ROI, and data is expressed as the cumulative distribution of ROIs from the spheroid core, the standard deviation of the distribution, and the average of the 10 furthest ROIs from the spheroid core. Using the ROIs obtained from the spheroid invasion analysis, the mean fluorescent intensity from the CF-CMPs was measured at each ROI and normalized to the area of the ROI. Additionally, the background CF-CMP signal from the no cell control conditions was subtracted from the fluorescent signal intensity in order to generate a normalized CF-CMP signal resulting from collagen remodeling by MDA-MB-231s. The results are further normalized to the 0 mM CF-CMP conditions since an autofluorescent signal from the MDA-MB-231s was captured in these control conditions.

3.2.6 Statistical Analysis

Statistical significance was determined by one-way ANOVA, and results were considered statistically significant for $p < 0.05$. Analysis and data visualization were performed in GraphPad Prism 8.3.1.

3.3 Results

3.3.1 Collagen-Mimetic Peptides Do Not Interfere with TNBC Spheroid Invasion

I first wanted to investigate whether or not CF-CMPs would influence TNBC cell behavior in the spheroid model of invasion. The CF-CMP design employed in our study contains the amino acid sequence GEKGER, which is known to engage the $\alpha_2\beta_1$ integrin due to its

capacity for electrostatically stable triple helical conformation, thereby allowing integrin recognition similar to native collagen[37]. Therefore, I sought to determine whether this sequence affected the invasive potential of our MDA-MB-231 cells by incorporating a percentage of the total collagen I content as CF-CMPs. We pre-incubated the collagen I and CF-CMP mixture at 4°C for at least 2 hours in order to allow the CF-CMPs to incorporate into the collagen I backbone prior to polymerization. Upon adding the mixture to our spheroid cultures, we allowed the gels to polymerize at 37°C and cultured the spheroids for 4 days before imaging. Based on the standard deviation of the spheroid distribution and the average of the 10 furthest points from the spheroid core, CF-CMPs were not shown to promote or inhibit cell invasion into the collagen I matrix, indicating that at these levels, CF-CMPs do not appear to be interacting with cells directly to an extent that elicits enhanced adhesion or invasion (Figure 4).

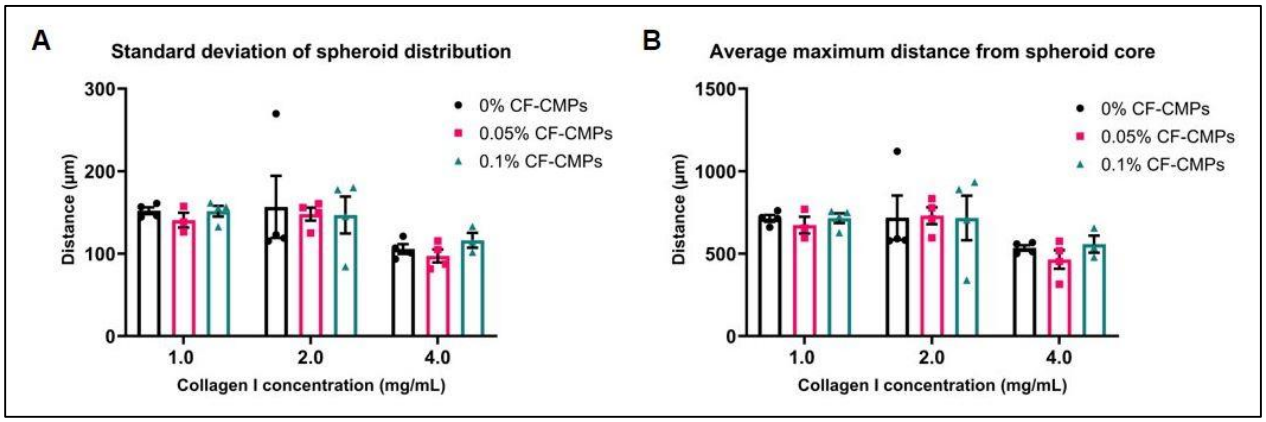

Figure 4 Spheroid invasion is not affected by pre-incubated CF-CMPs

(A) Standard deviation of spheroid distribution from core for 0, 0.05, and 0.1% CF-CMP conditions in 1, 2, and 4 mg/mL collagen I gels on day 4 of spheroid culture. (B) Average of 10 furthest points from spheroid core for 0, 0.05, and 0.1% CF-CMP conditions in 1, 2, and 4 mg/mL collagen I gels on day 4 of spheroid culture. Data represents group means ± standard error of measurement with n = 4 technical replicates. ANOVA: n.s.

3.3.2 Collagen Degradation During Spheroid Invasion Is Sufficient to Incorporate Collagen-Mimetic Peptides

In combination with a highly metastatic TNBC spheroid model, I wanted to determine whether the extent of collagen remodeling in a range of collagen I densities was sufficient to enable CMP hybridization in areas of collagen remodeling. As previously described, protease-mediated migration is more important for cell invasion in higher density collagen gels where pore size is reduced[36]. I therefore tested CF-CMP hybridization in both 1 and 2 mg/mL fixed gels in order to compare hybridization in both low and high levels of collagen degradation, respectively. Since CMPs have previously been applied to fixed 3D collagen gel samples[23], I first explored CF-CMP binding in fixed spheroid samples. After 2 hours of 5 mM CF-CMP incubation followed by thorough washing, significant CF-CMP hybridization was demonstrated in the 2 mg/mL collagen I gels (Figure 5A, 5B). Spheroid invasion analyses revealed that the extent of cell invasion into the 2 mg/mL collagen gel was significantly less than the 1 mg/mL gel (Figure 5C, 5D). These results indicate that collagen remodeling is elevated in higher density collagen gels, and that this level of degradation is sufficient for CMP hybridization in fixed samples.

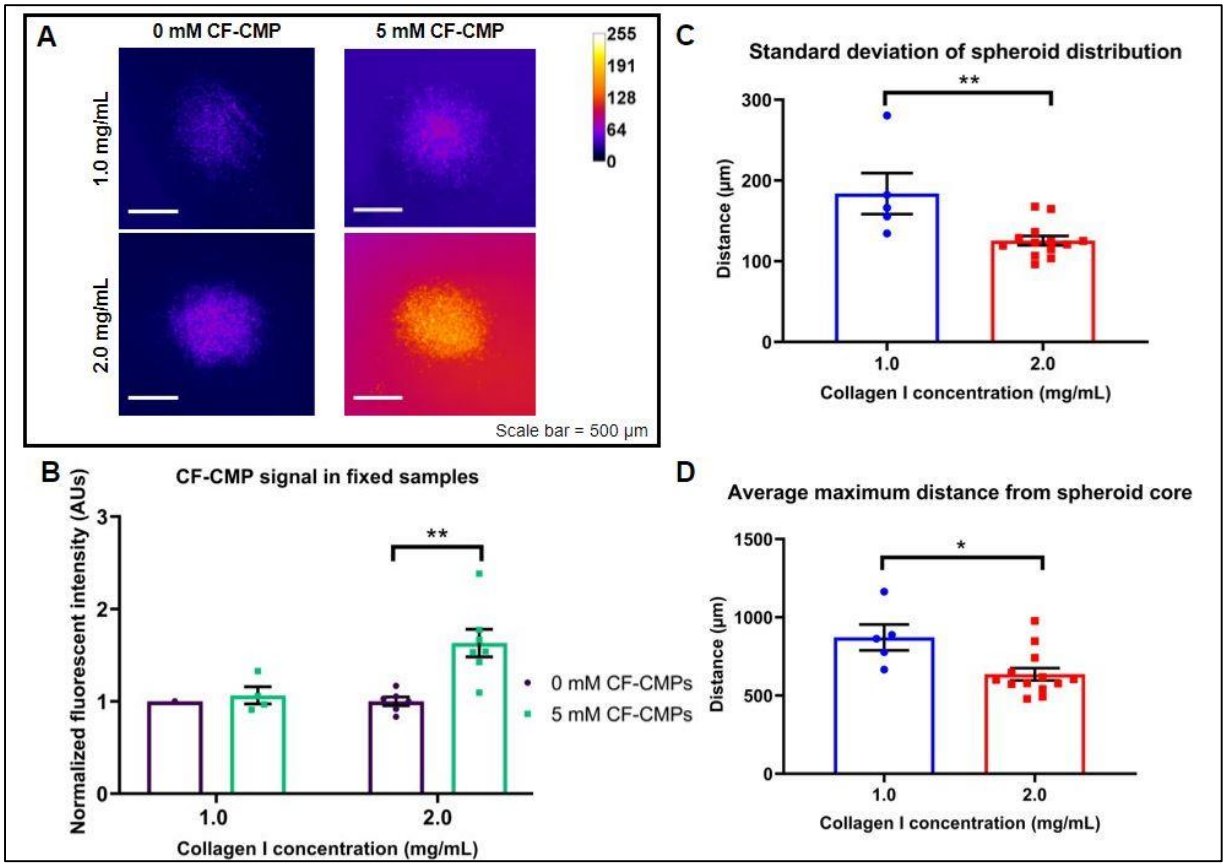

Figure 5 Collagen-mimetic peptides hybridize to areas of collagen degradation in fixed samples

(A) Representative pseudocolor images of CF-CMP signal using ImageJ fire look-up table (LUT) on day 4 in fixed 1 or 2 mg/mL collagen I gels. (B) Normalized CF-CMP signal intensity for 0 mM and 5 mM CF-CMP conditions relative to 0 mM control for 1 and 2 mg/mL collagen I gels. (C) Standard deviation of spheroid distribution from core for 0mM and 5mM CF-CMP conditions in 1 and 2 mg/mL collagen I gels on day 4 of spheroid culture. (D) Average of 10 furthest points from spheroid core for 0mM and 5mM CF-CMP conditions in 1 and 2 mg/mL collagen I gels on day 4 of spheroid culture. Data represents group means ± standard error of measurement with n = 2 biological replicates. Statistical significance ($p < 0.05$ or $p < 0.005$) from an unpaired Student's t-test is indicated by * or **, respectively.

3.3.3 Collagen-Mimetic Peptides Fail to Incorporate into Live Spheroids

The long-term clinical outlook of this project is to apply CMPs as vehicles for targeted drug delivery. Therefore, I sought to assess the binding capabilities of CF-CMPs in live spheroid samples in order to determine how well the CMPs hybridize in the presence of protease activity

and cellular uptake. I assessed the hybridization of CF-CMPs in live samples, incubated at 37°C, and compared the signal to fixed samples, incubated at 4°C, at 2 hours of CF-CMP incubation followed by thorough washing. In addition, I attempted to circumvent the differences in incubation temperature that could lead to reduced CF-CMP hybridization by incubating CF-CMPs for a longer time period of 24 hours since fluorescent CMP signal has been shown to increase with staining time in fixed tissue sections[26]. At 2 hours of CF-CMP incubation, the 5 mM signal increased relative to the 0 mM control, but not to a statistically significant extent (Figure 6A, 6B). A longer incubation time of 24 hours not only did not improve the CF-CMP signal, but actually resulted in a decrease in CF-CMP signal relative to the 2-hour incubation time. Compared to fixed samples, the extent of CF-CMP hybridization is reduced (Figure 6C). Given that CF-CMPs could hybridize in fixed samples, where CMPs were heated above the T_m and cooled to 4°C during hybridization, but did not work in live samples that were maintained at 37°C, I hypothesize that the temperature dependence of CF-CMP binding kinetics inhibits its application in live spheroids. Furthermore, the signal is shown to decay over longer incubation periods, indicating that CF-CMP hybridization is also impacted by live cell activity.

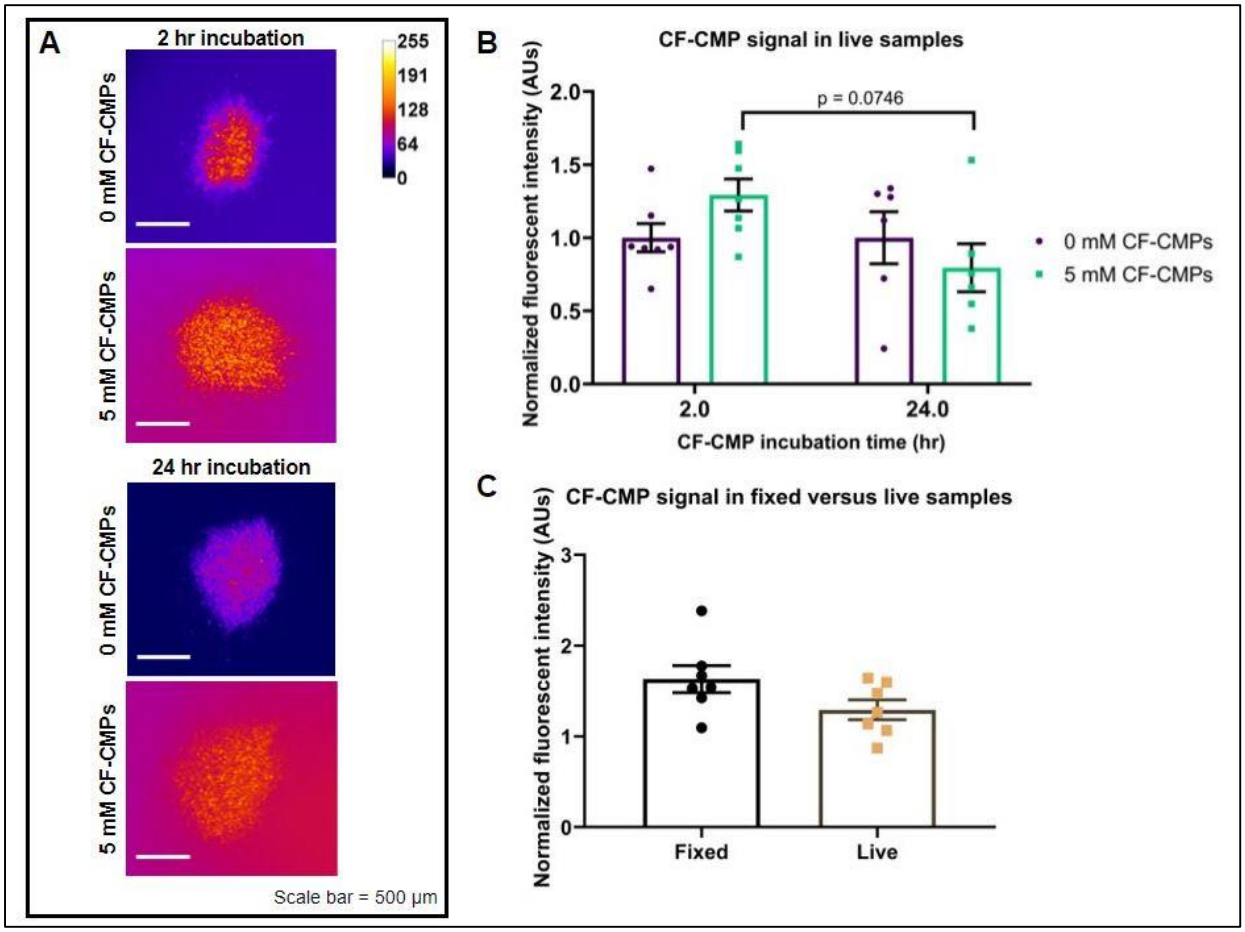

Figure 6 Collagen-mimetic peptide hybridization is reduced in live samples

(A) Representative pseudocolor images of CF-CMP signal using ImageJ fire look-up table (LUT) on day 4 in a live 2 mg/mL collagen I gel incubated for 2 or 24 hr. (B) CF-CMP signal intensity for 0 mM and 5 mM CF-CMP conditions in 2 mg/mL collagen I gels after 2 or 24 hr of CF-CMP incubation. (C) CF-CMP signal intensity relative to 0 mM control for fixed and live samples. Data represents group means ± standard error of measurement with n = 2 biological replicates. ANOVA: n.s.

3.4 Discussion

Previously, CMPs have been applied to fixed tissue samples in order to visualize areas of collagen turnover *in situ* using isolated tissue sections as well as *in vitro* using 3D models of collagen degradation[23,26]. Notably, the latter incorporated MDA-MB-231 cells into a 3D collagen

matrix to visualize collagen remodeling in the periphery of single cells[23]. I therefore sought to validate the use of CMPs in fixed spheroid samples in order to expand this application into live samples. To my knowledge, this is the first application of CMPs in the context of TNBC spheroid models. These results demonstrate that CMPs can be applied to fixed TNBC spheroid models, but this method could not be applied to live spheroids maintained at a temperature of 37°C.

Collagen-mimetic peptides containing bioactive sequences such as the glycine-glutamic acid-arginine (GER) triplet have been previously shown to bind the $\alpha_2\beta_1$ integrin, resulting in integrin-mediated cell adhesion, spreading, and proliferation in human mesenchymal stem cells[37,38]. The CF-CMP sequence employed herein contains this GEKGER sequence, resulting in an electrostatically stable triple helical conformation that enables integrin recognition. I therefore assessed the impact of CF-CMPs on MDA-MB-231 invasion by substituting 0, 0.05, or 0.1% of the total collagen I content as CF-CMPs in the ECM mixture added to spheroids on day 0. Over a period of 4 days, these levels of CF-CMPs had no impact on spheroid invasion according to metrics of the spheroid distribution. However, the effects of CF-CMPs should be reevaluated at higher concentrations to exacerbate any effects on TNBC spheroid invasion.

In fixed spheroid samples, a 5 mM solution of CF-CMPs incubated for 2 hours followed by several rounds of washing resulted in significant hybridization of the CF-CMPs in the direct vicinity of the cell spheroid. It is important to note that there is evidence of weak background GFP signal in the 0 mM control conditions due to autofluorescence of the MDA-MB-231 cells. I therefore first subtracted the background fluorescence of the gel for a given condition using a no cell control to correct for any background fluorescence the CMP may emit prior to hybridization. Next, I normalized the fluorescent intensity values to those of cells with no added CMP to

control for any autofluorescent signal from the cells. Interestingly, despite obvious cell invasion into the surrounding matrix seen in 1 mg/mL collagen I gels, there was no significant hybridization of the CF-CMPs in these low-density gels. This result is consistent with the finding that proteolytic remodeling of the ECM is less important for migration in lower density collagen gels since cells are able to migrate through larger pore sizes and therefore rely less on collagen degradation[36]. Furthermore, compared to the previously reported DQ-Col1 signal, the CF-CMP signal was able to capture evidence of collagen degradation in moderately dense 2 mg/mL gels, whereas the DQ-Col1 signal was only significant in higher density 4 mg/mL collagen gels. This finding indicates that CF-CMPs could provide a potentially more sensitive way of visualizing collagen remodeling than DQ-Col1.

Translating the administration of CF-CMPs from fixed spheroids to live spheroids entailed eliminating the temperature change that induced CMP hybridization. In fixed spheroid models, the CF-CMPs are thermally dissociated at 65°C, followed by cold quenching, administration, and incubation at 4°C. In live spheroids, this incubation temperature is 37°C. Although this temperature is below the melting temperature of 52°C the CF-CMP design, the net temperature change is reduced from 61°C to 15°C, thereby influencing the folding kinetics of the peptide. As a result, there is no significant hybridization of the CF-CMP signal in live spheroid samples at 2 hours.

Additionally, I analyzed the hybridization of CF-CMPs incubated for 24 hours in live samples in order to determine whether longer incubation times would improve binding of the peptide. As opposed to enhancing the CF-CMP signal, the longer incubation time actually resulted in a decay of the signal at 24 hours relative to 2 hours. In a previous study, CMPs were found to be internalized by cells via endocytosis after 5 days of incubation[29]. The finding in this

study that CF-CMP signal decays over a 24-hour incubation period indicates that cells are potentially internalizing the CF-CMPs, but further studies are required.

3.5 Conclusion

Here I used a spheroid model of highly metastatic TNBC in order to validate the hybridization of collagen-mimetic peptides in areas of collagen remodeling. CF-CMPs were found to have no effect on spheroid invasion, and to hybridize into areas of collagen degradation in moderately dense collagen gels in fixed samples. In translating the application of CF-CMPs from fixed to live spheroid samples, the signal was found to be reduced due to higher incubation temperatures, and therefore did not significantly hybridize in live samples, but evidence of slightly elevated CF-CMP signal warrants further investigation in different temperature settings. Finally, the CF-CMP signal was reduced over longer incubation periods, indicating that the signal is not retained in the gel, but potentially internalized by cells. Taken together, this work lays the foundation for analyzing CF-CMP localization to areas of collagen remodeling in TNBC models, and supports continued work on optimizing CF-CMP application in live spheroids in order to assess the delivery and retention of the signal in the presence of cells.

4 Conclusions and Future Directions

4.1 Conclusions

This work sought to examine the relationship between TNBC cell invasion and collagen degradation in order to assess the targeting capability of fluorescently-labeled CMPs in the TNBC tumor microenvironment. This was accomplished using a 3D spheroid of TNBC cells embedded in a collagen I matrix. Our lab previously demonstrated that this 3D spheroid culture was a strong predictive model of cell invasion[17], but this project aimed to determine whether 3D spheroids could also be used to model collagen degradation in higher density collagen I gels. These results demonstrate that spheroid invasion increases with collagen I density (Figure 2), and that higher collagen I densities also enhance collagen degradation according to the FITC DQ-Col1 signal (Figure 3). These methods provide an avenue for determining what mode of cell invasion occurs in our spheroid model depending on the density of the collagen matrix. Additionally, the optimized application of DQ-Col1 to our spheroid models can be used in the future to visualize collagen remodeling in these various contexts.

Additionally, this project established the use of fluorescently-labeled CMPs in TNBC spheroid models for the first time. Due to the GEKGER integrin-binding sequence contained in the CMP design, I first determined that CMPs do not impact spheroid invasion at low concentrations over the course of 4 days of growth (Figure 4). Building on a previous application of a similar CMP design to models of MDA-MB-231 cell-induced collagen remodeling in fixed 3D cell matrices[23], I determined the optimal fixing method, CF-CMP concentration, and washing regime in order to assess whether CMPs could hybridize to denatured collagen in fixed spheroid samples. The results indicate that a 5 mM CMP solution is sufficient to enable CMP

hybridization to areas of collagen remodeling in 2 mg/mL collagen I gels after 4 days of spheroid growth (Figure 5). This finding allows us to build off of these techniques in order to assess CMP hybridization in various contexts of spheroid invasion. Additionally, this work posits CMPs as a more sensitive tool for visualizing collagen degradation compared to DQ-Col1 since CMPs were able to capture collagen degradation in lower density collagen I gels.

Finally, this work sought to apply fluorescently-labeled CMPs to live spheroid samples in order to assess the delivery and retention of CMPs in TNBC microenvironments. Regardless of incubation time, our findings suggest that CMP hybridization is impaired in live samples due to the change in net temperature difference during CMP hybridization in fixed samples versus live samples, and that CMPs may start to be internalized after 24 hours of incubation in live spheroids (Figure 6). Further work is required to elucidate the refolding kinetics of the CMP design at various temperatures in order to determine the temperature cues required for hybridization. Ultimately, this project lays the foundation for eventually applying CMPs in live spheroid samples to determine how well CMPs are delivered and can target the TNBC tumor microenvironment, in addition to how long the CMPs are retained in the ECM before cellular internalization.

4.2 Future Directions

In identifying where CMPs are accumulating relative to TNBC cells, as well as assessing internalized CMPs, future work using higher magnification or confocal imaging is required. Second harmonic generation could also be used to visualize the triple helical content and fiber alignment of our collagen gels to study their role in cell invasion and collagen remodeling. Further assessment of the correlation between spheroid invasion and collagen degradation could

be supplemented by the use of protease inhibitors to suppress protease activity, or known stimulators of MMP production such as TNF-α to exacerbate protease-dependent remodeling[23,28]. These methods could also be applied to study the correlation between collagen degradation and CMP hybridization. In addition, other stromal cell types could be included in the spheroid culture in order to capture the role of stromal-derived proteases in collagen remodeling[10]. Moreover, future studies could attempt to incubate CMPs in live spheroids at room temperature in order to improve the extent of CMP hybridization. Although this method may not be applicable to *in vivo* studies, successful administration of CMPs in live spheroids will be useful for further elucidating the delivery and retention of CMPs in the presence of protease activity and cellular uptake. For *in vivo* studies, future work can apply CMPs systemically to animal models of TNBC tumors in order to determine how well the CMPs accumulate at tumor sites and where the off-target effects are occurring. Finally, beyond the context of cancer, CMPs can be applied to other models of pathogenic collagens including in the case of fibrosis, atherosclerosis, or other cancers to visualize collagen turnover or to target sites for therapeutic delivery.

5 References

1. Triple-Negative Breast Cancer. *American Cancer Society* (2019). Available at: https://www.cancer.org/cancer/breast-cancer/understanding-a-breast-cancer-diagnosis/types-of-breast-cancer/triple-negative.html. (Accessed: 15th April 2020)

2. Muschler, J. & Streuli, C. H. Cell-matrix interactions in mammary gland development and breast cancer. *Cold Spring Harb. Perspect. Biol.* **2**, 1–18 (2010).

3. Oskarsson, T. Extracellular matrix components in breast cancer progression and metastasis. *Breast* **22**, (2013).

4. Bonnans, C., Chou, J. & Werb, Z. Remodelling the extracellular matrix in development and disease. *Nature Reviews Molecular Cell Biology* **15**, 786–801 (2014).

5. Ossovskaya, V. *et al.* Exploring Molecular Pathways of Triple-Negative Breast Cancer. *Genes and Cancer* **2**, 870–879 (2011).

6. Kuczek, D. E., Hübbe, M. L. & Madsen, D. H. Internalization of Collagen: An Important Matrix Turnover Pathway in Cancer. in *Extracellular Matrix in Tumor Biology* (eds. Rolf A. Brekken & Dwyane Stupack) 17–38 (Springer, 2017). doi:10.1007/978-3-319-60907-2_2

7. Levental, K. R. *et al.* Matrix Crosslinking Forces Tumor Progression by Enhancing Integrin Signaling. *Cell* **139**, 891–906 (2009).

8. Provenzano, P. P. *et al.* Collagen density promotes mammary tumor initiation and progression. *BMC Med.* **6**, 1–15 (2008).

9. Martin, L. J. & Boyd, N. F. Mammographic density. Potential mechanisms of breast cancer risk associated with mammographic density: Hypotheses based on epidemiological evidence. *Breast Cancer Res.* **10**, 1–14 (2008).

10. Jodele, S., Blavier, L., Yoon, J. M. & DeClerck, Y. A. Modifying the soil to affect the seed: Role of stromal-derived matrix metalloproteinases in cancer progression. *Cancer Metastasis Rev.* **25**, 35–43 (2006).

11. Conklin, M. W. *et al.* Aligned collagen is a prognostic signature for survival in human breast carcinoma. *Am. J. Pathol.* **178**, 1221–1232 (2011).

12. Provenzano, P. P. *et al.* Collagen reorganization at the tumor-stromal interface facilitates local invasion. *BMC Med.* **4**, 1–15 (2006).

13. Shoulders, M. D. & Raines, R. T. Collagen structure and stability. *Annu. Rev. Biochem.* **78**, 929–958 (2009).

14. Yu, S. M., Li, Y. & Kim, D. Collagen mimetic peptides: Progress towards functional applications. *Soft Matter* **7**, 7927–7938 (2011).

15. Li, Y. *et al.* Direct detection of collagenous proteins by fluorescently labeled collagen mimetic peptides. *Bioconjug. Chem.* **24**, 9–16 (2013).

16. Hwang, J., Sullivan, M. O. & Kiick, K. L. Targeted Drug Delivery via the Use of ECM-Mimetic Materials. *Front. Bioeng. Biotechnol.* **8**, 1–19 (2020).

17. Baskaran, J. P. *et al.* Cell shape, and not 2D migration, predicts extracellular matrix-driven 3D cell invasion in breast cancer. *APL Bioeng.* **4**, (2020).

18. Hassiotou, F. & Geddes, D. Anatomy of the human mammary gland: Current status of knowledge. *Clin. Anat.* **26**, 29–48 (2013).

19. Kumar, S. & Weaver, V. M. Mechanics, malignancy, and metastasis: The force journey of a tumor cell. *Cancer Metastasis Rev.* **28**, 113–127 (2009).

20. Payne, S. L., Levin, M. & Oudin, M. J. Bioelectric Control of Metastasis in Solid Tumors. *Bioelectricity* **1**, 114–130 (2019).

21. Mah, E. J., Lefebvre, A. E. Y. T., McGahey, G. E., Yee, A. F. & Digman, M. A. Collagen density modulates triple-negative breast cancer cell metabolism through adhesion-mediated contractility. *Sci. Rep.* **8**, 1–11 (2018).

22. Wang, A. Y., Mo, X., Chen, C. S. & Yu, S. M. Facile modification of collagen directed by collagen mimetic peptides. *J. Am. Chem. Soc.* **127**, 4130–4131 (2005).

23. Bennink, L. L. *et al.* Visualizing collagen proteolysis by peptide hybridization: From 3D cell culture to in vivo imaging. *Biomaterials* **183**, 67–76 (2018).

24. Wang, A. Y. *et al.* Spatio-temporal modification of collagen scaffolds mediated by triple helical propensity. *Biomacromolecules* **9**, 1755–1763 (2008).

25. 3Helix. Applications for Collagen Hybridizing Peptides. *3Helix*

26. Hwang, J. *et al.* In Situ Imaging of Tissue Remodeling with Collagen Hybridizing Peptides. *ACS Nano* **11**, 9825–9835 (2017).

27. Li, Y. *et al.* Targeting collagen strands by photo-triggered triple-helix hybridization. *PNAS* **109**, (2012).

28. Urello, M. A., Kiick, K. L. & Sullivan, M. O. A CMP-based method for tunable, cell-mediated gene delivery from collagen scaffolds. *J. Mater. Chem. B* **2**, 8174–8185 (2014).

29. Urello, M. A., Kiick, K. L. & Sullivan, M. O. ECM turnover-stimulated gene delivery through collagen-mimetic peptide-plasmid integration in collagen. *Acta Biomater.* **62**, 167–178 (2017).

30. Luo, T., He, L., Theato, P. & Kiick, K. L. Thermoresponsive self-assembly of nanostructures from a collagen-like peptide-containing diblock copolymera. *Macromol. Biosci.* **15**, 111–123 (2015).

31. Luo, T. *et al.* Thermoresponsive Elastin-b-Collagen-Like Peptide Bioconjugate Nanovesicles for Targeted Drug Delivery to Collagen-Containing Matrices. *Biomacromolecules* **18**, 2539–2551 (2017).

32. Wolf, K. *et al.* Multi-step pericellular proteolysis controls the transition from individual to collective cancer cell invasion. *Nat. Cell Biol.* **9**, 893–904 (2007).

33. Balduyck, M. *et al.* Specific expression of matrix metalloproteinases 1, 3, 9 and 13 associated with invasiveness of breast cancer cells in vitro. *Clin. Exp. Metastasis* 171–178 (2000). doi:10.1023/A

34. Wu, P. H. *et al.* Particle tracking microrheology of cancer cells in living subjects. *Mater. Today* **39**, 98–109 (2020).

35. Wishart, A. L. *et al.* Decellularized extracellular matrix scaffolds identify full-length collagen VI as a driver of breast cancer cell invasion in obesity and metastasis. *Sci. Adv.* **6**, (2020).

36. Fraley, S. I. *et al.* Three-dimensional matrix fiber alignment modulates cell migration and MT1-MMP utility by spatially and temporally directing protrusions. *Sci. Rep.* **5**, 1–13 (2015).

37. Krishna, O. D., Jha, A. K., Jia, X. & Kiick, K. L. Integrin-mediated adhesion and proliferation of human MSCs elicited by a hydroxyproline-lacking, collagen-like peptide. *Biomaterials* **32**, 6412–6424 (2011).

38. Reyes, C. D. & Garcı, J. Engineering integrin-specific surfaces with a triple-helical collagen-mimetic peptide. (2002).